

## PROTOTYPE OF Ag@ZnO CORE SHELL FOR THE STERILIZATION OF MURAL PAINTINGS

Abeer Fouad EIHAGRASSY<sup>1\*</sup>, Sameh H. ISMAIL<sup>2</sup>

<sup>1</sup> Fayoum University, Faculty of Archaeology, Conservation Department,  
Fayoum University squar, 63514, Fayoum, Egypt.

<sup>2</sup> Cairo University, Faculty of Science, Faculty of Nanotechnology and Geologist,  
University Street, 12613, Giza, Egypt.

### Abstract

Cultural heritage sites often experience the unfavorable alteration of biodeterioration of mural paintings and wall inscriptions. Controlling or preventing biodegradation that may occur has been achieved through the use of various treatment methods, such as physical, chemical, and environmental control procedures. Regrettably, these treatments are often highly toxic to the health of conservators and visitors. Moreover, it causes pigmentation, is expensive, has low long-term results, and has poor long-term effectiveness. The use of Ag@ZnO core shell prototype in the field of cultural heritage was the first time in this research. The application was made to a painted wall inscription that dates back to the Middle Kingdom of ancient Egypt. A one-step chemical method was used to synthesize Ag@ZnO and it was examined using XRD, TEM, BET surface area, and Raman. These tests proved that the silver's core shell covered the zinc oxide's core and confirmed its purity. The painting on the wall was analyzed by SEN-EDX, Raman, and XRD analysis, and it was determined that the stone was limestone, the pigments were (Carbon for black pigment, Hematite for a red pigment, and Egyptian blue for blue pigment). These pigments and animal glue were combined to create the binding medium. The painted wall inscription was treated with Ag@ZnO treatments using a spray technique with a 5% concentration. The spectrophotometer was used to confirm that the color change has been below 5. This treatment method is non-hazardous, can be utilized both in vivo and in vitro, and does not necessitate the required environmental atmosphere or UV index.

**Keywords:** Nano Zinc Oxide; Nano silver; Core/shell; Sterilization; Painted wall inscription; Cultural heritage; Biodeterioration

### Introduction

Nanotechnology has been considered a multidisciplinary branch of science for the past two decades, and it has led to various concerns. Due to its versatility, it can be used in various scientific fields, including biomedical, pharmaceutical, agricultural, and environmental. Nanotechnology has been utilized in advanced materials, chemical sciences, physics, electronics, information technology, and similar subject areas, such as cultural heritage [1-5].

Nanostructures that contain a core and a shell are called core-shell nanostructures. One material can be used for the inner core, but a different material can be used for the shell. The shell core nanostructures of the crust are significant because they can enhance physical and chemical properties, leading to improved interaction on its surface, stability, and durability [6, 7].

\* Corresponding author: afa01@fayoum.edu.eg

Core-shell nanostructures' synthesis and design are influenced by two factors: the mix of the inner core material, the case shell material, and its face energy. If both elements have a high face energy, the shell-core nanostructure won't form, but the composite will form [8, 9].

In many industrial fields, the Ag nanoparticle is widely used as an anti-bacterial, anti-viral [10, 11], and anti-inflammatory nanoparticle [12]. Chemical, physical, and green techniques have been utilized to implement various synthesis methodologies or fabrication methods for silver nanoparticles [13,14]. Precipitation [15], hydrothermal [16] and sonochemical [17] are examples of these methods. Silver nanoparticles become yellowish when exposed to UV radiation, despite their great importance, causing a major issue for cultural heritage [18]. ZnO nanoparticles play an antibacterial role in wastewater treatment, historical painting sterilization, medicine, and bioremediation [19-22]. Consequently, there have been multiple approaches taken to synthesize zinc oxide. As well as the methods of precipitation [23], hydrothermal [24], and sonochemical [25], there are also green syntheses and ecofriendly processes [26, 27]. Nanoparticles have a range of unique properties, including optical-electrical properties [28], electronic properties [29], and photocatalytic properties [30] associated with the Ag@ZnO core/shell, metal core @ metal oxide shell. The thickness and discipline of the shell layer determine the chemical and physical properties of these materials, which is worth mentioning [31]. It is employed as an antibacterial to finish the disinfection process of bacteria such as *E. coli* and *S. aureus* within 60 to 90 minutes respectively at 35°C and in 45 to 60 minutes at 55°C. [32].

Biodeterioration of mural paintings is a significant factor in the destruction of cultural heritage [33,34]. Microbes have a significant impact on the decomposition of mural paintings; they are mechanically transported through the hypha [35, 36]. Chemically, metabolism is the process [37]. The painted layer's patina and pigments can be discolored by aesthetic damages that occur [38]. Numerous methods have been utilized to manage this deterioration factor, but unfortunately, most of these methods have shortcomings and could result in further decay [39-41].

An innovative nanotechnology technique called Ag@ZnO core/shell was utilized by us in this research paper. The methodology of microbial inhibition is novel because there hasn't been any research paper conducted using it in the field of cultural heritage. A simple one-step chemical method was used to synthesize the core/shell structures of Ag@ZnO. It was employed to prevent certain microbes that typically cause harm to wall inscriptions or mural paintings.

## Experimental part

### *Media: Malt extract agar*

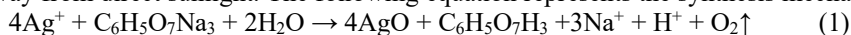
The preparation process for this media was based on [42,43] and involved the use of Malt extract 20g. L<sup>-1</sup>, Peptone 10g. L<sup>-1</sup>, Glucose 20g. L<sup>-1</sup>, Agar 20g. L<sup>-1</sup>, and Distilled water 1L. The pH medium was adjusted at 5.5.

### *Materials*

Oxford Company, India produced all of the chemicals used, including Zinc Acetate 99%, Absolute Ethanol 99.9%, Silver Nitrate and Tri-Sodium Citrate, which are analytical grade.

### *Synthesis of silver Nano-particles*

Precipitation is used to synthesize nano-particles and silver nano-particles that are reduced by tri-sodium citrate (TSC) [44]. 50mL of deionized double-distilled water is heated to boiling, resulting in the dissolution of 0.001M of AgNO<sub>3</sub>. By dripping, 0.01M of TSC drop is applied until the color turns pale yellow. Lastly, allow the solution to cool at room temperature and away from direct sunlight. The following equation represents the synthesis mechanism:



### ***Synthesis of ZnO Nano-particles***

The Zinc Acetate Dehydrate was dissolved in 50mL double-distilled water before being supplemented with 0.1M NaOH. At a rate of 300 rpm, slowly drop the solution and stir it until it turns white at room temperature. The final procedure was to dry the samples at 90°C for 2 hours and centrifuge them at 14,000rpm to produce ZnO nano-particles [45].

### ***Synthesis of Ag@ZnO core-shell Nanostructure***

The solution will become transparent when AgNO<sub>3</sub> is added to 1g in 50mL of deionized double-distilled water and stirred for 30 minutes at 80°C. At an output of 200w, 40kHz, at an amplitude of 80%, and seaweed involved in 0.75 cycles, add 0.1M Tri-Sodium Citrate solution to Ultrasound treatments until a light brown color appears. Afterward, allow the solution to cool at room temperature for an hour. Water distillation is used to create Ethanol by adding it to 0.1M Zinc Acetate and stirring for 30 minutes in the presence of 0.1% sodium hydroxide. This solution is mixed with 25mL of silver nano-particle dispersion solution and 50mL is added in total. Then, it was placed under 200W at 40kHz, with a capacity of 75%, and performed 0.5 cycles using seaweed for 3 hours at 60°C. One day has passed since the precipitated filter was ground and dried with air.

### ***Methods***

#### ***X-Ray diffractometry (XRD)***

Bruker's D8 model company carried out XRD to identify minerals. Reflectometry, high-resolution diffraction, IP-GID, SAXS, and investigations of residual stress and texture are all part of this research.

#### ***Transmission Electron Microscopy (TEM)***

The core-shell's morphology identification was determined through TEM using a high-resolution transmission electron microscope. The Japanese HR-TEM, also known as the EM-2100, was used for this experiment with 25x magnification and 200kV voltage.

#### ***X-ray Fluorescence (XRF)***

Using the X-Met 8000, an XRF instrument model from Oxford Instrument Company, elements in the Ag@ZnO shell core were identified.

#### ***BET surface area and pore size analysis***

The Nova Touch LX2 Surface Area and Pore Volume Analyzer model, which is made by Quanta Chrome in the USA, was used to analyze the surface area and pore volume.

#### ***Atomic Force microscopy (AFM)***

The surface topography and roughness profiles of nanomaterials were determined through the use of 2D and 3D AFM images acquired through the 5600LS model from Agilent Technology Company (USA).

#### ***Zeta potential***

The NanoSight NS500 instrument in Malvern, UK was utilized to analyze zeta potential data and determine the value, size, and surface charge of nanoparticulates.

#### ***Raman spectrometry***

The shape of particles of different colors can be seen in 2D and 3D confocal images. The chemical composition is determined by Raman spectroscopy using 3 different laser sources: 325, 532, and 785nm, and each color represents one of the chemical structures that make up the materials.

#### ***Identification of fungi***

Morphological studies at the microanalysis center at Cairo University were used to identify the fungal strains.

#### ***Spectrophotometry***

SDL Company has provided a manual for the Color EY E-3100 spectrophotometer.

## Results

### *Structure and characterization of Ag@ZnO*

#### *X-ray diffraction analysis*

The identification peaks of the ZnO and Ag nanoparticles were found to be free of any impurities or shifts by analyzing the Ag@ZnO core shell using XRD. ZnO peaks on the Ag nanoparticles are determined by the pattern, and the shell-core nanostructure has a strong interlayer interaction (Fig. 1).

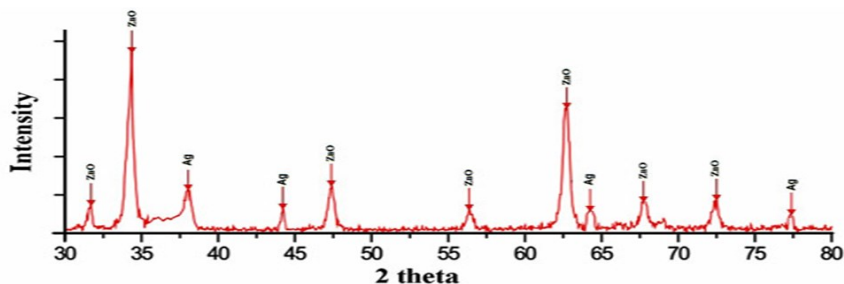


Fig. 1. The XRD spectrum of Ag@ZnO core shell

#### *Transmission Electron Microscope*

The Ag@ZnO core/shell is characterized by a shell of silver nanoparticles that are spherical-shaped and coated with ZnO, which is clearly visible in TEM images. The inner core has a size of 7 to 10 nanometers and a shell range of 1 to 3 nanometers. The Ag@ZnO core@shell nanostructure is sized between 8 and 13 nanometers. The distribution of particle size was well sorted, with particles having the same size and shape (Fig. 2).

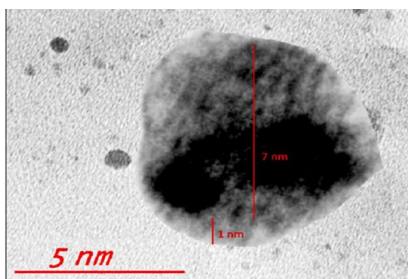


Fig. 2. Micro spherical silver nanoparticles coated in ZnO have an outer shell that is clear.

#### *X-ray Fluorescence*

The Ag@ZnO core shell nanostructure's chemical composition is confirmed by the XRF pattern to be pure, and the intensity of silver nanoparticles is greater than that of ZnO nanoparticles (Fig. 3).

#### *BET surface area*

The use of N<sub>2</sub> adsorption-desorption properties to determine surface area of silver nanoparticles, ZnO nanoparticles, and Ag@ZnO core shell nanostructures was utilized for different methods of surface area determination. To determine surface area, surface area can be determined using single/multiple BET methods, V-t Micro-porous method, External surface by V-t method, Langmuir, BJH adsorption-desorption, and DH adsorption-desorption methods. BJH sorption is used to determine the size of the pore for cumulative small and cumulative micro pores. Both the cumulative micro pore volume and cumulative pore volume for DH adsorption are taken into account. (Fig. 4, 5), and Table 1 displays the results.

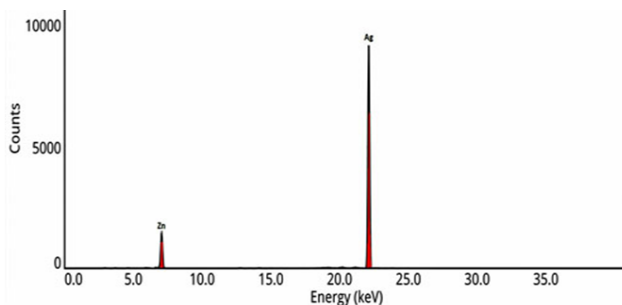


Fig. 3. The XRF spectrum of the Ag@ZnO core shell

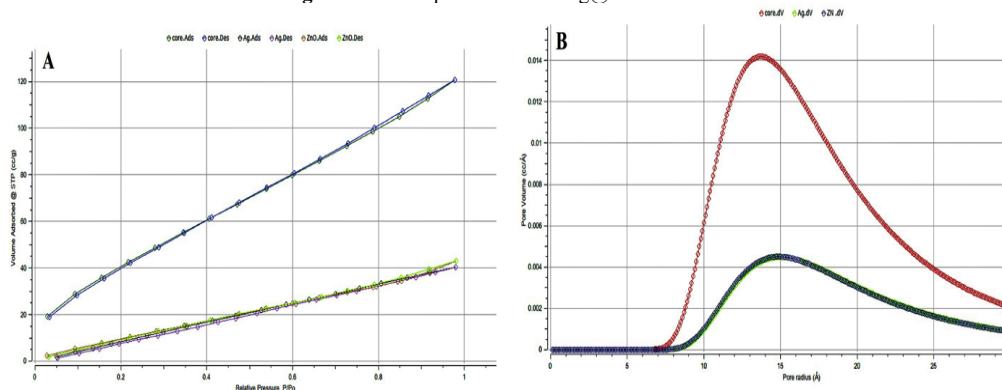


Fig. 4. The isotherm curve for silver Nano particles, ZnO Nano particles, and Ag@ZnO core shell nanostructure Silver nanoparticles, ZnO nanoparticles, and Ag@ZnO core shell nanostructure contain different pore volumes, by DH N<sub>2</sub> adsorption – micro-pore volume cumulative desorption method

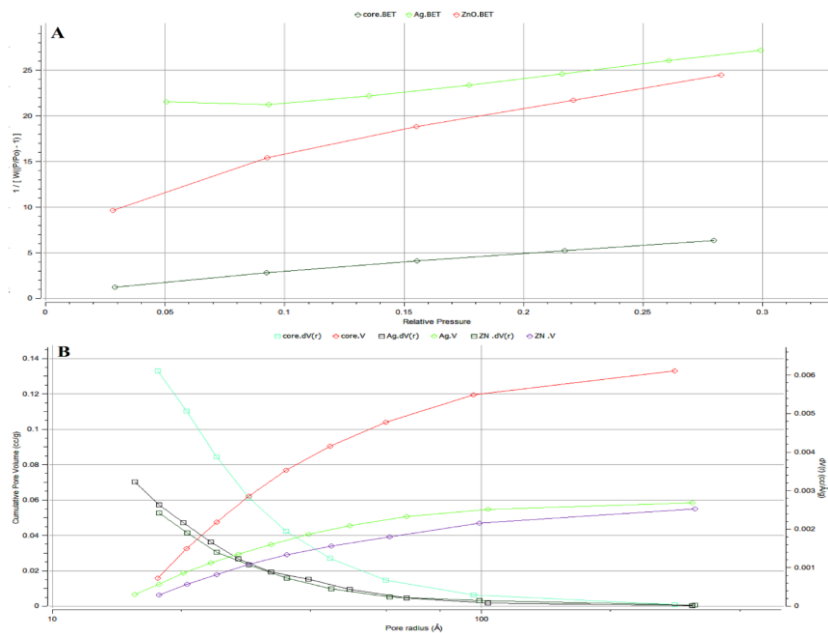


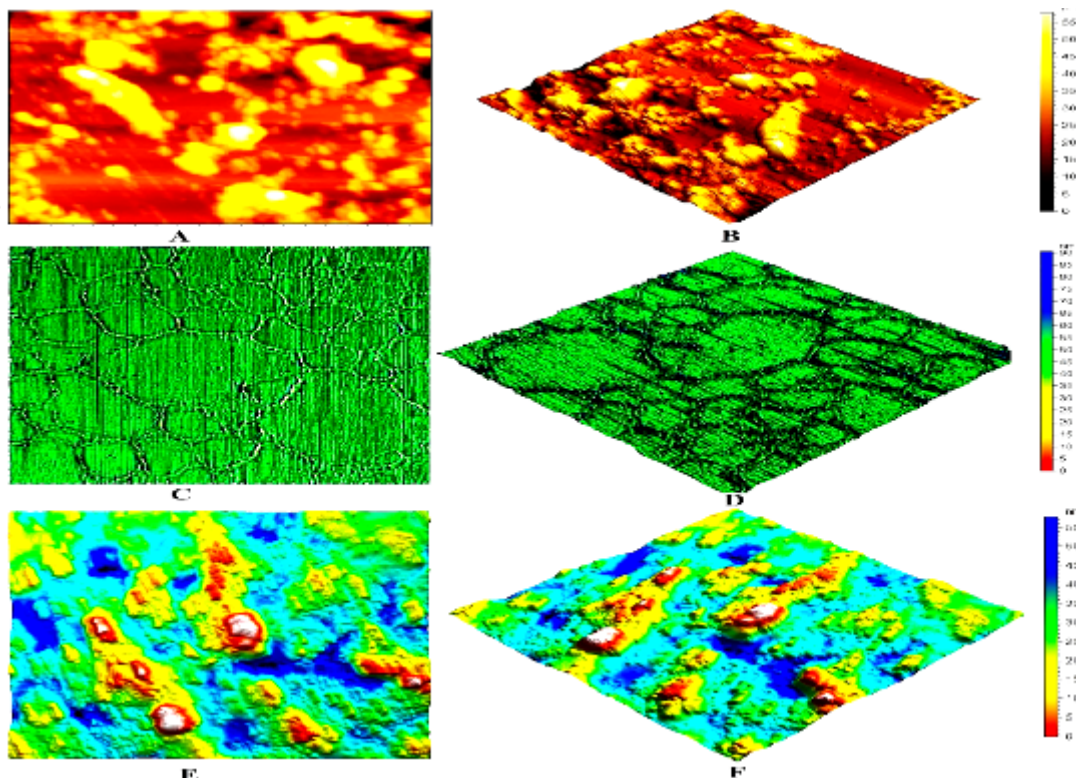
Fig. 5. The surface area determined by multivariate BET analysis of silver nanoparticles, ZnO nanoparticles, and Ag@ZnO core shell nanostructure. Adsorption of cumulative silver nanoparticles with small pore size using BJH, ZnO nanoparticles, and Ag@ZnO core shell nanostructure.

**Table 1.** Summary of the results of the surface area and pore volume analysis.

Parameters	Ag NPs m <sup>2</sup> /g	ZnO NPs m <sup>2</sup> /g	Core-shell m <sup>2</sup> /g
Single point BET surface area	38.2953	40.1748	152.575
Multipoint BET surface area	78.5218	52.9586	165.194
Langmuir method surface area	171.6	114.602	262.337
BJH adsorption surface area	40.6371	30.6278	79.9933
BJH desorption surface area	38.4854	40.2061	80.7746
DH adsorption surface area	41.7812	31.5488	82.4271
DH desorption surface area	39.3373	41.4203	83.2075
V-t method micro-pore surface area	39.1427	13.9529	84.3292
V-t method external surface area	39.3791	39.0056	80.8644
BJH adsorption cumulative micro-pore volume	0.0585583cc/g	0.0549862cc/g	0.132953cc/g
BJH desorption cumulative micro-pore volume	0.0583842cc/g	0.0620456cc/g	0.132933cc/g
DH adsorption cumulative micro-pore volume	0.0575669cc/g	0.0541036 cc/g	0.130959cc/g
DH desorption cumulative micro-pore volume	0.0570984cc/g	0.0610995cc/g	0.130939cc/g
V-t method micro-pore volume	0.00394228cc/g	0.00484738cc/g	0.0593941cc/g
Total pore volume	0.0624091cc/g	0.06365cc/g	0.187053cc/g

*Atomic Force Microscope*

AFM images and data analysis were utilized for the study of the roughness profile, spacing, surface topography, and pore volume. The purpose of this study is to examine the surface topography of silver nanoparticles, ZnO nanoparticles, and Ag@ZnO core-shell nanostructure. Ag, ZnO, and Ag@ZnO were applied to a thin sheet of archaeological pigment using a Spanish coating instrument. Fig. 6 and Table 2 display the results of the AFM image.



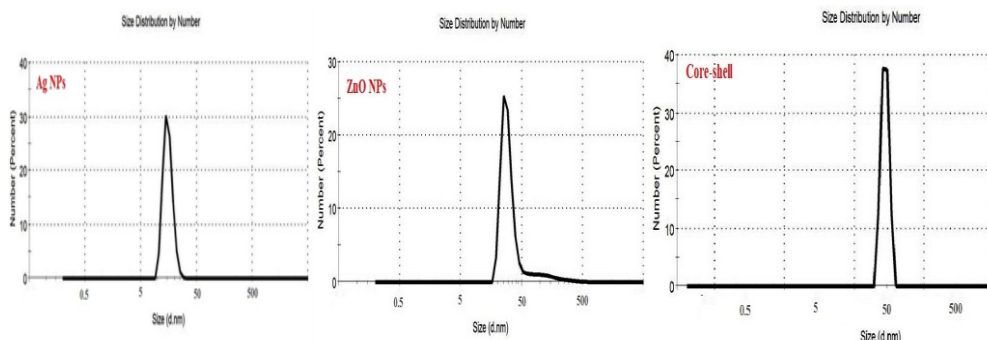
**Fig. 6.** Illustration of AFM images 5X5 Micron: A - Top view of silver nanoparticles; B - 3D view of silver nanoparticles; C - Top view of ZnO nanoparticles; D - 3D view of ZnO nanoparticles; E - Top view of Ag@ZnO core-shell nanostructure; F - 3D view of Ag@ZnO core-shell nanostructure (please enhance quality – numbers not visible)

**Table 2.** Illustrates AFM Amplitude parameters of silver Nano particle, ZnO Nano particles, and Ag@ZnO core shell nanostructure after application on the samples models.

Amplitude parameters – roughness profile				
Parameters	Ag NPs (Nm)	ZnO NPs (nm)	Core-shell (nm)	Description
Rp	11.1	18.3	56.7	Maximum peak height of roughness profile
Rv	16.1	22.4	40.2	Maximum Valley height of roughness profile
Rz	27.1	40.7	96.4	Maximum height of roughness profile
Rc	8.66	13.6	39.4	Mean height of roughness profile elements
Rt	27.1	40.7	96.4	Total height of roughness profile
Ra	2.21	3.18	11.4	Arithmetic mean height deviation of roughness profile
Rq	3.11	4.83	14.8	Root mean square height deviation of roughness profile
Rsk	-0.458	-0.49	0.299	Skewness of roughness profile
Rku	5.65	6.70	3.46	Kurtosis of roughness profile

*Zeta potential*

The Zeta sizer instruments were utilized to measure the size and zeta potential of silver nanoparticles, ZnO nanoparticles, and Ag@ZnO core shell nanostructures. The results of size and zeta potential are depicted in (Fig. 7) and Table 3.



**Fig. 7.** Illustrated the zeta size of silver Nano particle, ZnO Nano particles and Ag@ZnO core - shell nanostructure

**Table 3.** illustrated the zeta size and potential of silver Nano particle, ZnO Nano particles and Ag@ZnO core shell nanostructure

Parameters	Ag NPs	ZnO NPs	Core-shell
Size	8.0nm	45.3nm	58.6nm
Zeta potential	-51.3mV	-35.7mV	-21.4mV

*Raman spectroscopy*

The Raman shift of silver Nano particle, ZnO Nano particles and Ag@ZnO core shell nanostructure and 2D and 3D confocal image illustrated in (Fig. 8).

*Structure of the painted stone*

Fragments were taken from stone and pigments of the painted wall relief.

The XRD analysis showed that stone was Calcite according to the reference code (01-076-2916) consisting of 99% of Calcium Carbonate (CaCO<sub>3</sub>) and 1% of Quartz (SiO<sub>2</sub>) according to the reference code 01-086-2237 (Fig. 9).



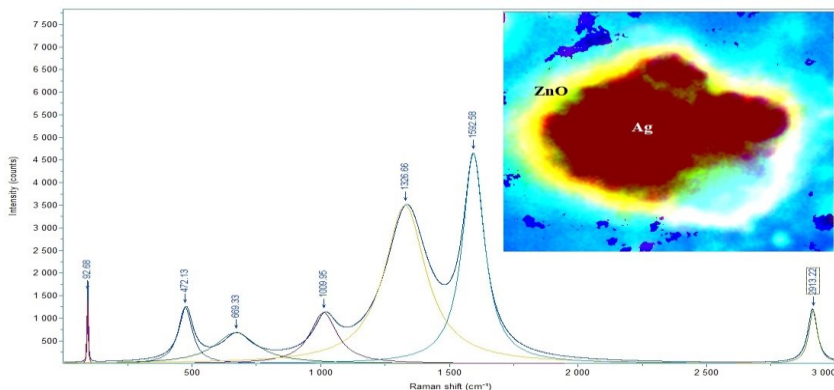


Fig. 8. Illustrated 2D confocal image and Raman shift of Ag@ZnO core-shell nanostructure inside the sample pours

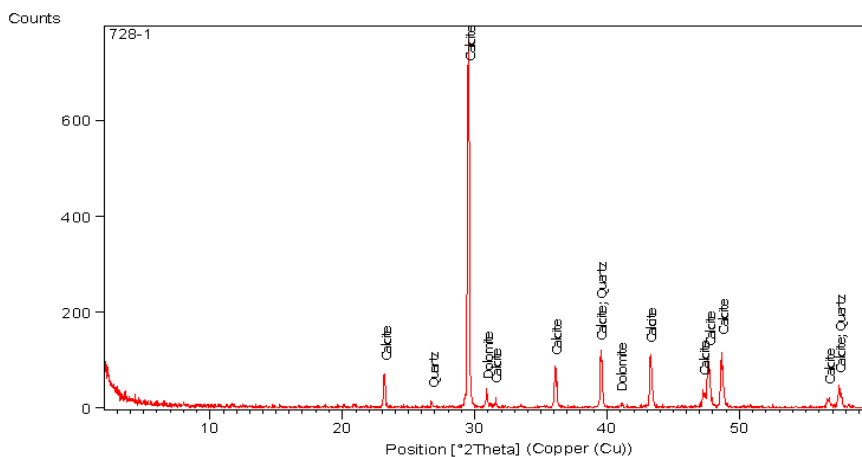


Fig. 9. The XRD spectrum of stone wall inscription

Fragments of the pigments were characterized by SEM-EDX not by XRD due to its small size that cannot be examined by XRD. The Analysis showed that, the black pigment was Carbon - C deteriorated by Halite - NaCl (Fig.10), while the red pigment was Hematite - Fe<sub>2</sub>O<sub>3</sub> (Fig. 11) and the blue pigment was Egyptian blue - CaCuSi<sub>4</sub>O<sub>10</sub> (Fig. 12).

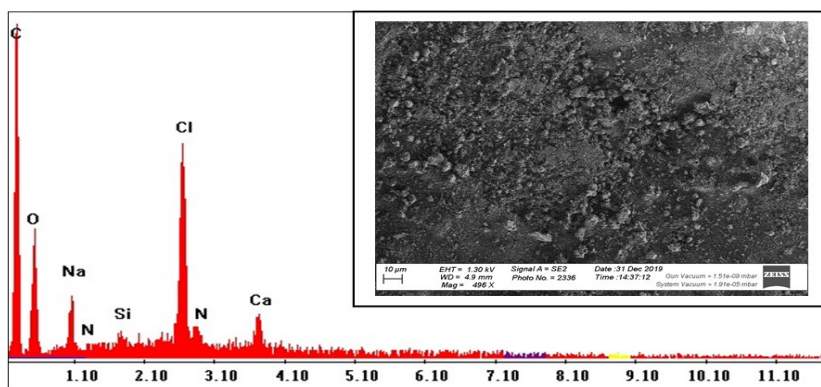


Fig. 10. Represents the spectrum of black pigment



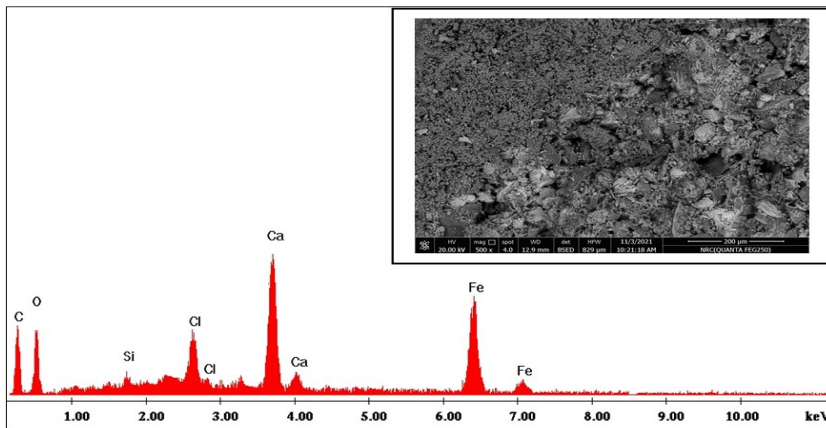


Fig. 11. Represents the spectrum of red pigment

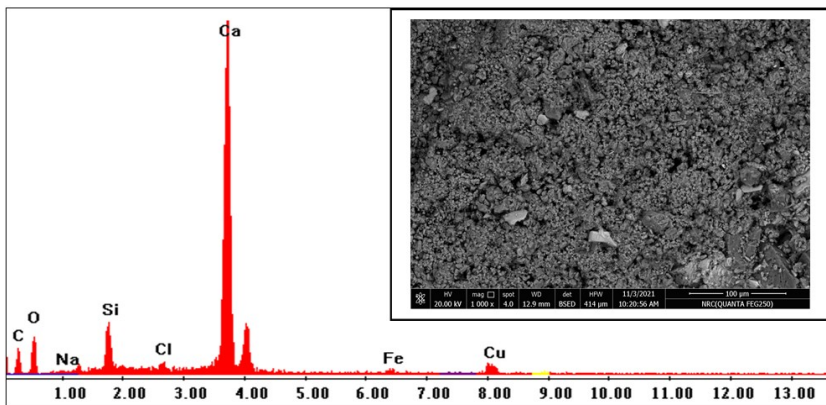


Fig. 12. shows the spectrum of Egyptian blue pigment

Raman spectra presented a slight degree of Animal glue used as a binding media. The sample showed the spectrum of calcite with strong peaks at  $260.93$  and  $1088.92\text{cm}^{-1}$ , black carbon the main peaks at  $1319.55$  and  $1587.93\text{cm}^{-1}$  and animal glue spectrum with main peaks  $649.92$ ,  $1003.94$ ,  $1374.41$  and  $1587.35\text{cm}^{-1}$  (Fig. 13).

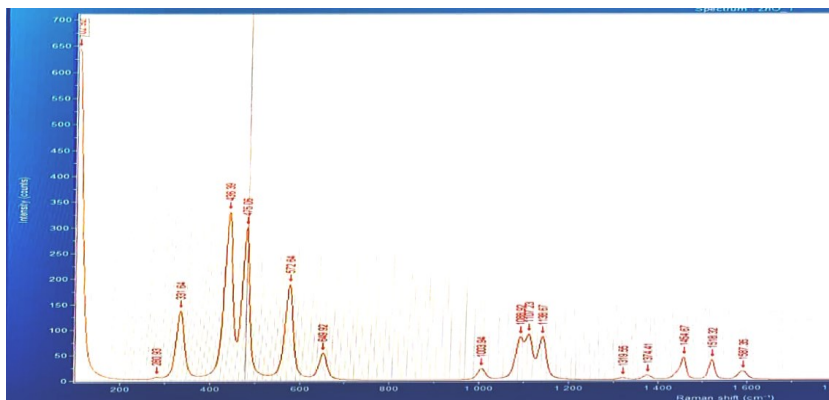


Fig. 13. Shows the Raman spectrum of the binding media

### ***Deterioration Factors***

The painted wall inscription was affected by many missing parts, strong dust particles conjoined with pigments, and after cleaning the surface many spots of iron oxide were scattered all over the stone, the EDX was indicated the presence of Halite although it not cleared by neck eyes (Fig. 14).



Fig. 14. Shows the missed parts, the dust particles, and the spotty iron oxides

### ***Identification of Fungi***

According to the morphological studies conducted by the microanalysis center at Cairo University (Table 4), *Aspergillus niger*, *Aspergillus flavus*, *Rizopus stolonifer*, *Pencillium cyclopium*, caused the painted wall inscription to deteriorate.

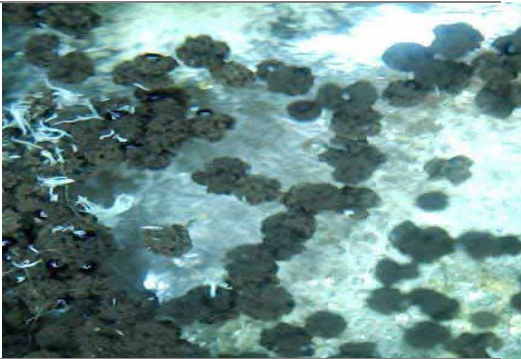
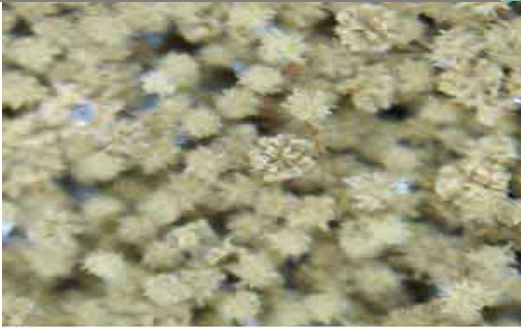
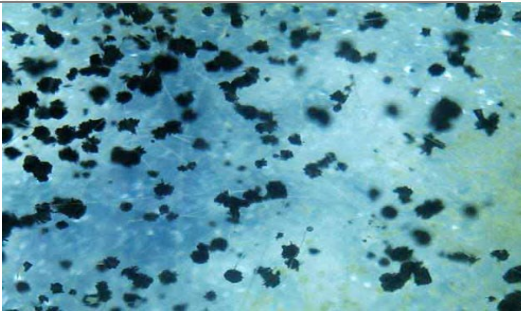

### ***Ag@ZnO anti- microbial effect***

Petri dishes were used to culture the control strains of *Aspergillus niger*, *Aspergillus flavus*, *Rhizopus stolonifer*, and *Pencillium cyclopium* in malt extract media. The antimicrobial activity of Ag@ZnO was determined by applying three concentrations (1, 3, and 5mL) to petri dishes cultured with one strain of fungi. The remaining petri dishes, each with a volume of 10mL of media and 5mL of Ag@ZnO core shell, were combined and cultivated with a dtrain of fungi. The incubation period for all petri dishes was 7 days at 25°C. As shown in Table 5, there was no colony growth after the incubation period.

### ***Applied Ag@ZnO on the wall inscription***


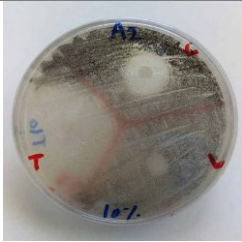
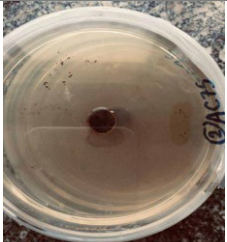

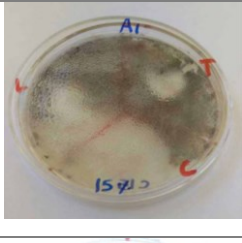
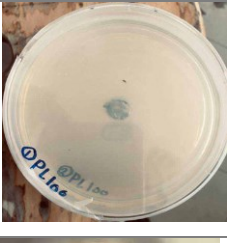
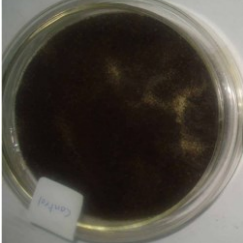
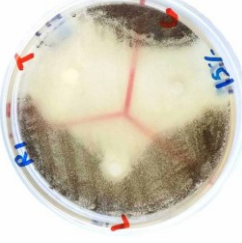
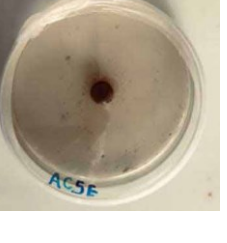
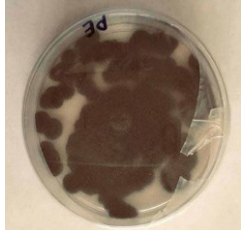
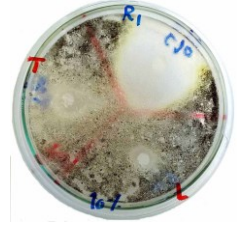

The pigments were coated with Ag@ZnO core shell using spray technique and allowed to dry at room temperature for four months before being analyzed by XRD. The analysis revealed that the Ag@ZnO core shell was still within the stone even after 120 days and was not accessible to the environment (Fig. 15).

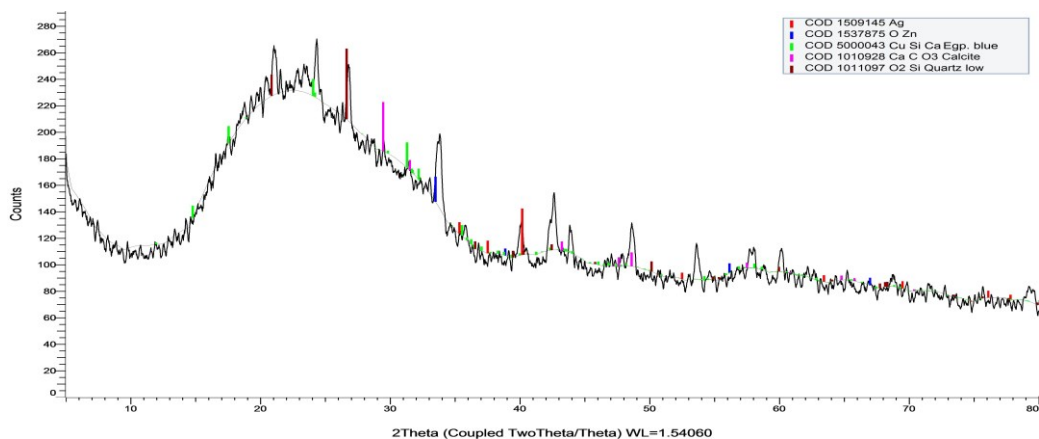
**Table 4.** The fungi examined by USB digital microscope

Microbes	Magnification	USB digital microscope image
<i>Aspergillus niger</i>	400x	
<i>Aspergillus flavus</i>	400x	
<i>Rhizopus stolonifer</i>	400x	
<i>Penicillium cyclopium</i>	400x	



**Table 5.** The growth of microbes before and after using Ag@ZnO

Microbes	Before	Anti-microbial effects	Mixed media with Ag@ZnO
<i>Aspergillus niger</i>			
<i>Aspergillus flavus</i>			
<i>Rhizopus stolonifer</i>			
<i>Penicillium cyclopium</i>			



**Fig. 15.** Presents the presence of Ag@ZnO coreshell inside the wall inscription grains after four months

**Spectrophotometer measuring** [46-49]

The treated wall inscription by Ag@ZnO coreshell was examined by spectrophotometer before and after four months of application (Table 6).

**Table 6.** The  $\Delta E^*$  of the painted wall inscription pigment before and after applied of Ag@ZnO core shell

Pigments	Before treatment			After four month			$\Delta E^*$
	$\Delta L^*$	$\Delta a^*$	$\Delta b^*$	$\Delta L^*$	$\Delta a^*$	$\Delta b^*$	
<i>Carbon</i>	40.45	-20.90	18.86	43.52	-21.01	19.25	3.09
<i>Hematite</i>	41.96	-13.56	19.33	43.75	-13.93	21.06	2.51
<i>Egyptian blue</i>	-50.20	-40.92	52.12	-53.74	-41.68	54.63	4.40

**Discussion**

Nanomaterials are being primarily studied for sterilization, with a primary focus on photocatalytic sterilization and synergistic sterilization with antibiotics [50,51]. It has been confirmed by the main characterization of the Ag@ZnO core-shell nanostructure and the individual silver and zinc oxide nano particles that the core-shell nanostructure was formed. The physical and chemical properties were examined and it was ultimately determined whether the new unique properties affect the Ag@ZnO core-shell nanostructure as an anti-microbial agent.

The synthesis of Ag@ZnO core-shell nanostructures was confirmed by XRD, Raman, and XRF results with no impurities from the synthesis method or shifted peak positions for both Ag and ZnO nanoparticles. The Ag@ZnO core-shell nanostructure's purity suggests that the ingestion of microbes is a direct result of its purity.

The TEM images demonstrate that the shell (ZnO) is well-coated on the core (Ag) and has a uniform shape and size. We investigated the direct effects of the shape and size of Nano Ag@ZnO core-shell nanostructure as anti-microbe agents based on its homogeneity. The surface area of materials that are anti-bacterial and fungicidal is crucial because of their tiny size. [52,53].

The Ag@ZnO core-shell nanostructure's antibacterial and anti-fungal action is enhanced by its larger surface area compared to individual silver nanoparticles and zinc oxide nanoparticles [54, 55]. Ag@ZnO's increased surface area compares with silver and zinc oxide nano particles, resulting in a greater surface charge distribution, which leads to a boost in fungus activity. Ag@ZnO's high surface area and pores with a capillary system and nano size make them highly chemically active and increase their surface charge. Ag@ZnO's anti-bacterial and anti-fungus properties are made efficient by its large surface area and surface charge, which facilitates faster and better interactions with microorganisms [56].

The zeta sizer was used to incorporate silver nanoparticles, zinc oxide nanoparticles, and Ag@ZnO core shell, and it was discovered that Ag@ZnO is larger than individual silver and zinc oxide nanoparticles. During the TEM image, it can be seen that the Ag@ZnO core-shell nanostructure is composed of silver and zinc oxide nanoparticles that are 1.0 and 7.0 nm in size, as shown by the image. Silver and zinc oxide nanoparticles in individual states are larger than this size. Ag@ZnO's small size is capable of penetrating the pours of stones without leaving any residue on the surface, regardless of their size. The utilization of it in various fields of cultural heritage and in different organic (narrow pours) or inorganic materials is enhanced by that advantage [57].

AFM scans of the sample model after application revealed an extensive roughness profile for the Ag@ZnO core-shell nanostructure, which surpasses the roughness profile of individual silver and zinc oxide nano-particles. By adhering to bacteria and fungus, this feature gives it an advantage as an anti-microbial [58].

XRD, Raman, and SEM-EDX were used to analyze the structure of wall inscription. The stone support's composition was determined by XRD analysis to consist of Calcite (Calcium

Carbonate) and a trace of Quartz. The wall inscription made of limestone, commonly used in the old and middle kingdom, is indicated by this result. The wall inscription dates back to the Middle Kingdom's beginning.

The pigment analysis presented that the black pigment was Carbon deteriorated by Halite salt's (NaCl), the red pigment was Hematite according to the presence of iron element (Fe), the blue pigment was the Egyptian blue according to the presence of Silicon (Si), Calcium (Ca), and Copper (Cu). *A. Lucas* [59]. The main peaks of 650, 1004, 1374, and 1587  $\text{cm}^{-1}$  [60] in the spectrum have been confirmed by Raman spectroscopy analysis as animal glue.

The antimicrobial effects analysis of using Ag@ZnO core shell were carried by applied three different concentration of the core shell (1, 3 and 5mL) on petri dishes inoculated by *Aspergillus niger*, *Aspergillus flavus*, *Rhizopus stolonifer*, *Pencillium cyclopium* and incubated for a week. According to the final results, the growth activity of whole microorganisms can be inhibited by a concentration of 5mL. confirming that the Ag@ZnO core shell has an antimicrobial effect. [61,62]

Despite four months of application, the pigments of the painted wall inscription were not affected by the Ag@ZnO core shell, as determined by the spectrophotometer analysis. the  $\Delta E^*$  was less than 5 and cannot be noticed by necked eyes. The core shell is benefitted by the slight color change, which provides a safe environment for pigments and the patina of stones. [63]. The archaeological stone sample's XRD analysis was prompted by the application of Ag@ZnO core shell for four months, confirmed that the Ag@ZnO core shell was not released in the environment as it was still in the pours.

## Conclusions

The main findings of the research paper are worth mentioning. Ag@ZnO core-shell nanostructures “particles that contain an inner core of Ag-coated by ZnO as a shell” that was used for sterilization and inhibitions of microorganisms. The importance of Core-shell nanostructures is to improve the physical and chemical properties that enhance the reactivity on its surface, its stability, and dispensability.

The Ag@ZnO core-shell has many advantages, its structures are synthesized by rapid, simple one-step sonochemical method, low cost, anti-microbial, and risk-free on the pigments. Ag@ZnO core-shell nanostructures have physical and chemical properties that are better than silver and zinc oxide Nano particles which effect bioactivity. The huge surface area and high roughness profile enable Ag@ZnO core-shell nanostructures for sterilization and inhibitions of microbes. Ag@ZnO core-shell nanostructures has the ability to inhibit *Aspergillus niger*, *Aspergillus flavus*, *Rhizopus stolonifer*, *Pencillium cyclopium* that were previously isolated from the painted wall inscription. The Ag@ZnO core-shell solves the problem of using Ag nanoparticles which affected by U.V. and lose its role for inhibition of microbes in addition to color the make noble patina yellowish. Only 5% of Ag@ZnO can be used as antimicrobial agent with effected period up to four months and can be used in vivo and in vitro.

It is hoped that such findings and recommendations are taken into consideration with an interest on using such a technique in the preservation of the mural paintings and painted stone inscription to remain a source of attraction to the tourists from all over the world.

## References

- [1] H. Devalapally, A. Chakilam, M.M. Amiji, *Role of Nanotechnology in Pharmaceutical Product Development*, **Journal of Pharmaceutical Sciences**, **96**, 2007, pp. 2547-2565.
- [2] W. Hannaha, P.B. Thompson, *Nanotechnology, risk and the environment: a review*, **Journal of Environmental Monitoring**, **10**, 2008, pp. 291-300.

- [3] M. Sharon, M.K. Choudhary, R. Kumar, *Nanotechnology in Agricultural Diseases and food safety*, **Journal of Phytology**, **2**, 2010, pp. 83–92.
- [4] G. Song, L. Cheng, Y. Chao, K. Yang, Z. Liu, *Emerging Nanotechnology and Advanced Materials for Cancer Radiation Therapy*, **Advanced Materials**, **29**, 2017, Article Number: 1700996.
- [5] A. Crous, H. Abrahamse, *Innovations in Nanotechnology for Biomedical Sensing, Imaging, Drug Delivery, and Therapy*, **Nanotoxicology**, (Editors: H.K. Daima, S.L. Kothari, & S.K. Bhargava), First edition, CRC Press, 2021, <https://doi.org/10.1201/9780429299742>.
- [6] R.G. Chaudhuri, S. Paria, *Core-shell nanoparticles: Classes, properties, synthesis mechanisms, characterization, and applications*, **Chemical Reviews**, **112**, 2012, pp. 2373–2433.
- [7] Y.R. Chen, H.H. Wu, Z.P. Li, *The study of surface plasmon in Au/Ag core/shell compound nanoparticles*, **Plasmonics**, **7**, 2012, pp. 509–513.
- [8] R. Zamiri, A. Zakaria, R. Jorf, *Laser assisted fabrication of ZnO/Ag and ZnO/Au core/shell nanocomposites*, **Applied Physics**, **111**, 2013, pp. 487–493.
- [9] J.G. Oh, H. Kim, *Synthesis of core-shell nanoparticles with a Pt nanoparticle core and a silica shell*, **Current Applied Physics**, **13**, 2013, pp. 130–136.
- [10] S. Galdiero, A. Falanga, M. Vitiello, M. Cantisani, V. Marra, M. Galdiero, *Silver Nanoparticles as Potential Antiviral Agents*, **Molecules**, **16**, 2011, pp. 8894–8918.
- [11] S. Karagoz, N.B. Kiremitler, G. Sarp, S. Pekdemir, S. Salem, A.G. Goksu, M.S. Onses, I. Sozdutmaz, E. Sahmetlioglu, E.S. Ozkara, A. Ceylan, E. Yilmaz, *Antibacterial, Antiviral, and Self-Cleaning Mats with Sensing Capabilities Based on Electrospun Nanofibers Decorated with ZnO Nanorods and Ag Nanoparticles for Protective Clothing Applications*, **ACS Applied Materials & Interfaces**, **13**, 2021, pp. 5678–5690.
- [12] K.M. Aparna Mani, S. Seethalakshmi, V. Gopal, *Evaluation of In-vitro Anti-Inflammatory Activity of Silver Nanoparticles Synthesised using Piper Nigrum Extract*, **Journal of Nanomedicine Nanotechnology**, **6**, 2015, DOI: 10.4172/2157-7439.1000268.
- [13] A. Wasilewska, U. Klekotka, M. Zambrzycka, G. Zambrowski, I. Swi ´ ecka, B. KalskaSzostko, *Physico-chemical properties and antimicrobial activity of silver nanoparticles fabricated by green synthesis*, **Food Chemistry**, **400**, 2023, pp. 133960. <https://doi.org/10.1016/j.foodchem.2022.133960>.
- [14] F.E. Ettadili, M. Azriouil, B. Chhaibi, F.Z. Ouattmane, O. Tahiri Alaoui, F. Laghriba, A. Farahi, M. Bakasse, S. Lahrich, M.A. EL Mhammedi, *Green synthesis of silver nanoparticles using Phoenix dactylifera seed extract and their electrochemical activity in Ornidazole reduction*, **Food Chemistry Advances**, **2**, 2023, pp. 100146.
- [15] P.W. Wu, B. Dunn, V. Doan, B. J. Schwartz, E. Yablonovitch, M. Yamane, *Controlling the Spontaneous Precipitation of Silver Nanoparticles in Sol-Gel Materials*, **Journal of Sol-Gel Science and Technology**, **19**, 2000, pp. 249–252.
- [16] M. Mostafa, *Synthesis of nanosilver by the hydrothermal method and its application for radioiodine sorption from alkaline solution*, **Journal of Radioanalytical and Nuclear Chemistry**, **304**, 2015, pp. 1153–1162.
- [17] B. Kumar, K. Smita, L. Cumbal, A. Debut, R.N. Pathak, *Sonochemical Synthesis of Silver Nanoparticles Using Starch: A Comparison*, **Bioinorganic Chemistry and Applications**, 2014, Article Number: 784268, DOI: 10.1155/2014/784268.
- [18] A. Adel, *Using nanomaterial in the treatment of the Biodeterioration of Limestone in Archaeological Building, Applied on one of the selected models*, **Master in Science Degree**, Fayoum University, 2021, p.213.
- [19] J. Sawai, *Quantitative evaluation of antibacterial activities of Metallic oxide powders (ZnO, MgO, and CaO) by conducti metric assay*, **Journal of Microbiological Methods**, **54**, 2003, pp. 177–182.



- [20] J. Sawai, T. Yoshikawa, *Quantitative evaluation of antifungal activity of metallic oxide powders (MgO, CaO, and ZnO) by an indirect conductimetric assay*. *Journal of Applied Microbiology* **96**, 2004, pp. 803-809.
- [21] J. Sawai, O. Yamamoto, B. Ozkal, Z.E. Nakagawa, *Antibacterial activity of carbon-coated zinc oxide particles*. *Biocontrol Science* **12**, 2007, pp. 15-20.
- [22] J. Kaszewski, P. Kielbik, E. Wolska, B. Witkowski, L. Wachnicki, Z. Gajewski, M. Godlewski, M.M. Godlewski, *Tuning the luminescence of ZnO: Eu nanoparticles for applications in biology and medicine*, *Optical Materials*, **80**, 2018, pp. 77-86.
- [23] P.M. Aneesh, K.A. Vanoja, M.K. Jayaraj, *Synthesis of ZnO nanoparticles by hydrothermal method*, *Nanophotonic Material, Proc. of SPIE*, **6639**, 2007, Article Number: 66390J· 0277-786X/07/\$18, DOI: 10.1117/12.730364.
- [24] H.R. Ghorbani, F.P. Mehr, H. Pazoki, B.M. Rahmani, *Synthesis of ZnO Nanoparticles by Precipitation Method*, *Orient Journal of Chemistry*, **31**, 2015, pp. 1216-1221.
- [25] A. Roy, S. Maitra, S. Ghosh, S. Chakrabarti, *Sonochemically synthesized iron-doped zinc oxide nanoparticles: Influence of precursor composition on characteristics*, *Materials Research Bulletin*, **74**, 2016, pp. 414-440.
- [26] A. Annapoorani, A. Koodalingam, M. Beulaja, G. Saiprasad, P. Chitra, A. Stephen, S. Palanisamy, N.M. Prabhu, S.G. You, S. Janarthanan, R. Manikandan, *Eco-friendly synthesis of zinc oxide nanoparticles using Rivina humilis leaf extract and their biomedical applications*, *Process Biochemistry*, **112**, 2022, pp. 192-202,
- [27] B. Mortezagholi, E. Movahed, A. Fathi, M. Soleimani, A.F. Mirhosseini, N. Zeini, M. Khatami, M. Naderifar, B. Abedi Kiasari, M. Zareanshahraki, *Plant-mediated synthesis of silver-doped zinc oxide nanoparticles and evaluation of their antimicrobial activity against bacteria cause tooth decay*, *Microscopy Research Tech.*, **85**, 2022, pp.3553–3564.
- [28] F. Li, J. Wua, Q. Qin, Z. Li, X. Huang, *A facile method to prepare monodispersed ZnO–Ag core-shell microspheres*, *Super Lattices Microstructure*, **47**, 2010, pp. 232–240.
- [29] M.S.S. Danish, A. Bhattacharya, D. Stepanova, A. Mikhaylov, M.L. Grilli, M. Khosravy, T. Senjyu, *A Systematic Review of Metal Oxide Applications for Energy and Environmental Sustainability*, *Metals Journal*, **10**, 2020, Article Number: 1604; DOI: 10.3390/met10121604
- [30] G. Maidecchi, V.D. Chinh, R. Buzio, A. Gerbi, G. Gemme, M. Canepa, F. Bisio, *Electronic Structure of Core-Shell Metal/Oxide Aluminum Nanoparticles*, *The Journal of Physical Chemistry*, **119**, 2015, pp. 26719–26725
- [31] X. Chen, Y. Lou, C. Burda, *Spectroscopic investigation of II–VI core-shell nanoparticles: CdSe/CdS*, *International Journal of Nanotechnology*, **1**, 2004, doi.org/10.1504/IJNT.2004.003721
- [32] S. Das, N. Ranjana, A.J. Misra, M. Suar, A. Mishra, A.J. Tamhankar, C.S. Lundborg, S.K. Tripathy, *Disinfection of Water Borne Pathogens Escherichia coli and Staphylococcus aureus by Solar Photocatalysis Using Sonochemically Synthesized Reusable Ag/ZnO Core-Shell Nanoparticles*, *International Journal of Environmental. Res. Public Health*, **14**, 2017, Article Number: 747; DOI: 10.3390/ijerph14070747.
- [33] A. ElHagrassy, *Isolation and characterization of actinomycetes from Mural paintings of Snu- Sert-Ankh tomb, their antimicrobial activity, and their biodeterioration*, *Microbiological research*, **216**, 2018, pp. 47-55.
- [34] A. Pyzik, K. Ciuchcinski, M. Dziurzynski, L. Dziewit, *The Bad and the Good Microorganisms in Cultural Heritage Environments an Update on Biodeterioration and Biotreatment Approaches*, *Materials*, **14**, 2018, Article Number: 177. <https://doi.org/10.3390/ma14010177>
- [35] K. Sterflinger, G. Piñar, *Microbial deterioration of cultural heritage and works of art tilting at windmills*, *Appl Microbiol Biotechnol*, **97**, 2013, pp. 9637–9646

- [36] X. Liu, R.J. Koestler, T. Warscheid, Y. Katayama, J.D. Go, *Microbial deterioration and sustainable conservation of stone monuments and buildings*, **Nature Sustainability**, **3**, 2020, pp. 991–1004.
- [37] A. Grottoli, M. Beccaccioli, E. Zoppis, R.S. Fratini, E. Schifano, M.L. Santarelli, D. Uccelletti, M. Reverberi M. *Nanopore Sequencing and Bioinformatics for Rapidly Identifying Cultural Heritage Spoilage Microorganisms*, **journal Frontiers in Materials**, **7**, 2020, DOI: 10.3389/fmats.2020.00014
- [38] D.S. Nitiu, A.C. Mallo, M.C.N. Saparrat, *Fungal melanins that deteriorate paper cultural heritage: An overview*, **Mycologia**, **112**, 2020, pp. 859-870.
- [39] T. Li, Y. Hu, H. Zhang, *Evaluation of efficiency of six biocides against microorganisms commonly found on Feilafeng Limestone, China*, **Journal of Cultural Heritage**, **43**, 2020, pp. 45-50
- [40] F. Cappitelli, C. Cattò, F. Villa, *The Control of Cultural Heritage Microbial Deterioration*, **Microorganisms**, **8**, 2020, Article Number: 1542. doi.org/10.3390/microorganisms8101542
- [41] G. Ranalli, E. Zanardini, *Bio-cleaning on Cultural Heritage: new frontiers of microbial biotechnologies*. **Journal of Applied Microbiology**, **131**, 2021, pp. 583-603
- [42] D. Smith, A.H.S. Onions, **The Preservation and Maintenance of Living Fungi**. Kew, Surrey: Common wealth Mycological Institute, 1983.
- [43] D. Smith, A.H.S. Onions, *A comparison of some preservation techniques for fungi*. **Trans. Br. Mycol. Soc.** **81**, 1983, pp. 535-540
- [44] S. Sajjad, A. Nasser, *Synthesis and stabilization of Ag nanoparticles on a polyamide surface and its antibacterial effects*, **International Nano Letter**, **1**, 2011, pp. 22-24
- [45] D. Osman, M. Mustafa, *Synthesis and Characterization of Zinc Oxide Nanoparticles using Zinc Acetate Dihydrate and Sodium Hydroxide*. **Journal of Nanoscience and Nanoengineering**, **1**, 2015, pp. 248-251.
- [46] J. Schanda, **Colorimetry**, Wiley-Interscience John Wiley & Sons Inc., 2007, p. 56.
- [47] G.V. Atodiressei, I.G. Sandu, E.A. Tulbure, V. Vasilache, R. Butnaru, *Chromatic characterization in CieLab system for natural dyed materials, prior activation in atmospheric plasma type DBD*, **Revista de Chimie (Bucharest)**, **64(2)**, 2013, pp. 165-169.
- [48] V. Pelin, I. Sandu, S. Gurlui, M. Branzila, V. Vasilache, E. Bors, I.G. Sandu, *Preliminary investigation of various old geomaterials treated with hydrophobic pellicle*, **Color Research and Application**, **41(3)**, 2016, pp. 317-320, Special Issue SI. DOI: 10.1002/col.22043.
- [49] A.M. Saviuc-Paval, A.V. Sandu, I.M. Popa, I.C.A. Sandu, A.P. Berteau, I. Sandu, *Colorimetric and Microscopic Study of the Thermal Behaviour of New Ceramic Pigments*, **Microscopy, Research and Technique**, **76(6)**, 2013, pp. 564-571, DOI: 10.1002/jemt.22201.
- [50] Y. Liu, F. Li, Z. Guo, Y. Xiao, Y. Zhang, X. Sun, T. Zhe, Y. Cao, L. Wang, Q. Lu, J. Wang, *Silver nanoparticle-embedded hydrogel as a photothermal platform for combating bacterial infections*, **Chemical Engineering Journal**, **382**, 2020, 122990, doi.org/10.1016/j.cej.2019.122990.
- [51] X. Zhang, G. Zhang, H. Zhang, X. Liu, J. Shi, H. Shi, X. Yao, P. K. Chu, X. Zhang, *A bifunctional hydrogel incorporated with CuS@MoS<sub>2</sub> microspheres for disinfection and improved wound healing*, **Chemical Engineering Journal**, **382**, 2020, 122849, doi.org/10.1016/j.cej.2019.122849.
- [52] O. Yamamoto, *Influence of particle size on the antibacterial activity of zinc oxide*. **International Journal of Inorganic Materials**, **3**, 2001, pp. 643-646.
- [53] W. Han, W. Wang, J. Fan, R. Jia, X. Yang, T. Wu, Q. Wu, *A novel Ag/ZnO core-shell structure for efficient sterilization synergizing antibiotics and subsequently removing*

- residuals*, **Green Energy & Environment**, 2022, <https://doi.org/10.1016/j.gee.2022.07.004>.
- [54] O.M. Elshayb, M.N. Abdelwahed, A.H. Sadek, S.H. Ismail, A. Shami, B.M. Alharbi, B.A. Alhammad, M. F. Seleiman, *The Integrative Effects of Biochar and ZnO Nanoparticles for Enhancing Rice Productivity and Water Use Efficiency under Irrigation Deficit Conditions*, **Plants**, **11**, 2022, pp. 1416. doi.org/10.3390/plants11111416.
- [55] A.N. Abdel Rahman, M.S. Shakweer, S.A. Algharib, A.I. Abdelaty, S. Kamel, T.A. Ismail, W.M. Daoush, S.H. Ismail, H.H. Mahboub, *Silica nanoparticles acute toxicity alters ethology, neuro-stress indices, and physiological status of African catfish (*Clarias gariepinus*)*, **Aquaculture Reports**, **23**, 2022, Article Number: 101034, doi.org/10.1016/j.aqrep.2022.101034.
- [56] G.K. Hassan, A. Abdel-Karim, M.T. Al-Shemy, Patricia Rojas, Jose L. Sanz, Sameh H. Ismail, Gehad G. Mohamed, Fatma A. El-gohary, Aly Al-sayed, *Harnessing Cu@Fe<sub>3</sub>O<sub>4</sub> core shell nanostructure for biogas production from sewage sludge: Experimental study and microbial community shift*, **Renewable Energy**, **188**, 2022, pp. 1059-1071.
- [57] S.T. El-Wakeel, A. Abdel-Karim, S.H. Ismail, G.G. Mohamed, *Development of Ag-dendrites @Cu nanostructure for removal of selenium (IV) from aqueous solution*. **Water Environment Research**, **94**, 2022, Article Number: e10713, doi.org/10.1002/wer.10713.
- [58] N.N.H. Shosha, S. Elmasry M. Moawad, S.H. Ismail, M. Elsayed, *In vivo and invitro evaluation of antitumor effects of iron oxide and folate core shell-iron oxide nanoparticles*, **Brazilian Journal of Biology**, **84**, 2022, doi.org/10.1590/1519-6984.253183.
- [59] A. Lucas, **Ancient Egyptian Materials and Industries**, Third edition, London: Edward Arnold, 1948, pp.125–27.
- [60] F. Casadio, C. Daher, L. Bellot-Gurlet, *Raman spectroscopy of Cultural Heritage materials: overview of applications and new frontiers in Instrumentation, sampling modalities, and data processing*, **Topics in Current Chemistry**, **374**, 2016, doi.org/10.1007/s41061-016-0061-z.
- [61] X. Huang, Y. Chen, X. Feng, X. Hu, Y. Zhang, L. Liu, *Incorporation of oleic acid-modified Ag@ZnO core-shell nanoparticles into thin film composite membranes for enhanced antifouling and antibacterial properties*, **Journal of Membrane Science**, **602**, 2020, 117956, <https://doi.org/10.1016/j.memsci.2020.117956>.
- [62] S. Anjum, K. Nawaza, B. Ahmad, C. Hano, B. H. Abbasi, *Green synthesis of biocompatible core-shell (Au–Ag) and hybrid (Au–ZnO and Ag–ZnO) bimetallic nanoparticles and evaluation of their potential antibacterial, antidiabetic, antiglycation and anticancer activities*, **Royal society of chemistry**, **12**, 2022, pp. 23845-23859
- [63] A. Plutino, G. Simone, *The limits of colorimetry in cultural heritage applications*, **Coloration Technology**, **137**, 2021, pp.56–63

---

Received: October 02, 2022

Accepted: August 24, 2023